

Timescape cosmology with radiation fluid

James A.G. Duley, M. Ahsan Nazer and David L. Wiltshire

Department of Physics and Astronomy, University of Canterbury, Private Bag 4800,
Christchurch 8140, New Zealand

Abstract. The timescape cosmology represents a potentially viable alternative to the standard homogeneous cosmology, without the need for dark energy. Although average cosmic evolution in the timescape scenario only differs substantially from that of Friedmann-Lemaître model at relatively late epochs when the contribution from the energy density of radiation is negligible, a full solution of the Buchert equations to incorporate radiation is necessary to smoothly match parameters to the epoch of photon decoupling and to obtain constraints from cosmic microwave background data. Here we extend the matter-dominated solution found in earlier work to include radiation, providing series solutions at early times and an efficient numerical integration strategy for generating the complete solution. The numerical solution is used to directly calculate the scale of the sound horizon at decoupling, and at the baryon drag epoch. The constraints on these scales from the Planck satellite data yield bounds on the timescape cosmological parameters, which are found to also agree with the best-fit values from a recent analysis of SDSS-II supernova data, while avoiding the problem of a primordial lithium-7 abundance anomaly.

PACS numbers: 98.80.-k, 04.20.Cv, 98.80.Jk, 98.80.Es

1. Introduction

The standard model of cosmology is based on the assumption that average cosmic evolution is identical to that of an exactly homogeneous isotropic Friedmann–Lemaître–Robertson–Walker (FLRW) model. This assumption is well justified at the epoch of last scattering, by the evidence of the Cosmic Microwave Background (CMB) radiation. However, small density perturbations eventually grow nonlinear, forming the observed structures of the universe, and by the present epoch the universe is only homogeneous in some average statistical sense when one averages on scales $\gtrsim 100 h^{-1}\text{Mpc}$, where h is the dimensionless parameter related to the Hubble constant by $H_0 = 100h \text{ km sec}^{-1} \text{ Mpc}^{-1}$. Below this scale we observe a universe dominated in volume by voids [1]–[3], with clusters of galaxies in walls, sheets and filaments surrounding and threading the voids.

The problem of fitting a smooth geometry to this complex hierarchical structure entails many fundamental issues [4]–[6], including in particular: (i) how is average cosmic evolution to be described; and (ii) how are local observables related to quantities defined with respect to some average geometry? There has been considerable interest in these problems in recent years (for some recent reviews see [6]–[10]) since it is possible that a full understanding of these issues might explain the observation of cosmic acceleration attributed to a smooth form of dark energy in the standard cosmology.

In this paper, we will focus on the timescape cosmology [11]–[13], which is a phenomenologically viable model of the universe to the extent that it has been tested [13]–[16]. The differences between the predictions of the timescape model and those of the Λ CDM model for supernova luminosity distances are at the same level as current systematic uncertainties in data reduction [15]. The timescape model fits the angular scale of sound horizon in the CMB anisotropy data, and the Baryon Acoustic Oscillation (BAO) scale in galaxy clustering statistics [14] but these tests have not yet been developed to the extent that they can tightly constrain cosmological parameters.

The timescape model is based on the Buchert scheme [17, 18] for statistical averages of a fully inhomogeneous geometry, while maintaining a statistical Copernican principle. Since the Buchert scheme involves statistical quantities, additional physical assumptions are required to relate its average parameters to cosmological observables [19, 20].

In the timescape model it is postulated that the relevant physical assumptions relate to gravitational energy: in particular, to the relative regional volume deceleration of expanding regions of different density, which provides a measure of the relative kinetic energy of regional expansion [11, 21]. In the absence of an exact timelike Killing vector, bound systems – which necessarily form in regions where the density is greater than critical – can always be embedded within expanding regions bounded by a “finite infinity surface” [4, 11, 21] within which the smoothed geometry is spatially flat, with a close to Einstein-de Sitter expansion law.

It is postulated that in describing the statistical cosmological geometry one can always choose a uniform Hubble flow slicing, akin to a constant mean extrinsic curvature (CMC) slicing, in which the effects of regional scalar spatial curvature are compensated

by the choice of the canonical time coordinate of “cosmological inertial frames”, namely expanding regions whose spatial extent is smaller than the (negative) curvature scale but larger than bound systems [21]. The canonical time parameter for observers within finite infinity regions, where galaxies and other bound systems are located, is then related to the time parameter appearing in the Buchert statistical averages by a phenomenological lapse function. By a procedure of matching null geodesics in the two geometries [11], solutions of the Buchert equations can be related to cosmological observables determined by observers (such as ourselves) within bound systems where the regional spatial curvature is different from the global statistical average.

The physical explanation of apparent cosmic acceleration in the timescape scenario relies then not simply on the backreaction of inhomogeneities which define the average cosmic evolution, but more on the differences of gravitational energy manifest in the canonical clocks of observers in galaxies as compared to observers in voids, where the spatial curvature is negative. These differences are insignificant in the early universe which is close to homogeneous, but the differences grow cumulatively and become especially large when voids come to dominate the volume of the universe. Phenomenologically, apparent acceleration is found to begin when the void fraction reaches 59% [11].

The timescape scenario faces two main challenges to be developed into a model that can fully compete with the standard Λ CDM cosmology:

- At a formal level new mathematical constructions are required to define a modified statistical geometry of the universe, and the methods by which it is patched to regional geometries. The procedures of coarse-graining, and their relationship to gravitational energy and entropy have to be well-understood.
- At an observational level, cosmological tests which rely heavily on the standard FLRW model in data reduction procedures need to be revisited from first principles. This applies in particular to the analysis of the power spectrum of CMB anisotropies, and to the analysis of galaxy clustering statistics.

The present paper will take steps towards the second of these goals by fully incorporating a radiation fluid in the solution of the Buchert equations.

At epochs prior to last scattering the universe is close to homogeneous, so that timescape model is almost indistinguishable from the standard cosmology. In previous work [11] estimates of the angular diameter distance of the sound horizon, and calibrations of the baryon-to-photon ratio for big bang nucleosynthesis, were made by simply matching the matter only solution of the Buchert equations to a spatially flat FLRW model with matter and radiation. While this may be sufficient for simple estimates, a more detailed treatment of cosmic evolution of the early universe after last scattering requires that the radiation component is incorporated directly.

2. Buchert equations for two-scale model with radiation fluid

Our primary aim in this paper is to extend the exact solution of [12, 13] to include the contributions of relativistic species (photons and neutrinos) directly in the solution of the Buchert equations. The matter content will therefore be taken as that of the standard cosmology without a cosmological constant, namely matter fields in the form of both baryonic and nonbaryonic matter treated as dust, plus photons and the standard three generations of neutrinos.

At early epochs when radiation is dominant the universe is assumed to be very close to homogeneous and isotropic, and thus the solution we expect will be very close to that of a standard matter plus radiation FLRW model with negligible spatial curvature. Furthermore at late epochs, when the solutions to the Buchert equations differ substantially from a FLRW model, the contribution of the radiation energy density to the overall energy density is negligible. At late epochs it is only the matter component which drives the overall evolution of the universe (assuming no dark energy), and it is the matter component which defines the density gradients. While the radiation fluid certainly responds to density gradients, this only affects questions such as gravitational lensing, rather than the average cosmological evolution considered here.

We will therefore treat the radiation fluid as a component with a pressure $P_R = \frac{1}{3}\rho_R$ which commutes under the Buchert average,

$$\partial_t \langle P_R \rangle - \langle \partial_t P_R \rangle = \langle P_R \theta \rangle - \langle P_R \rangle \langle \theta \rangle = 0, \quad (1)$$

throughout the evolution of the universe, rather than using the more detailed Buchert formalism that applies to fluids with pressure [18]. Here θ is the expansion scalar and angle brackets denote the spatial volume average of a quantity on the surface of average homogeneity, so that $\langle P_R \rangle \equiv \left(\int_{\mathcal{D}} d^3x \sqrt{\det {}^3g} P_R(t, \mathbf{x}) \right) / \mathcal{V}(t)$, where $\mathcal{V}(t) \equiv \int_{\mathcal{D}} d^3x \sqrt{\det {}^3g}$ is the average spatial volume, ${}^3g_{ij}$ being the 3-metric. The detailed Buchert formalism for general averaging and backreaction in fluids with pressure may be of relevance for deriving further results in a perturbation theory approach in the early universe. In this paper, however, we confine ourselves to finding a smooth solution which makes a transition from radiation domination to the late epoch matter-dominated solution of the timescape cosmology [11]–[13].

With our assumptions the radiation fluid does not contribute to the backreaction, and the Buchert equations [17, 18] may then be written

$$\frac{3\dot{\bar{a}}^2}{\bar{a}^2} = 8\pi G (\langle \rho_M \rangle + \langle \rho_R \rangle) - \frac{1}{2} \langle \mathcal{R} \rangle - \frac{1}{2} \mathcal{Q}, \quad (2)$$

$$\frac{3\ddot{\bar{a}}}{\bar{a}} = -4\pi G (\langle \rho_M \rangle + 2\langle \rho_R \rangle) + \mathcal{Q}, \quad (3)$$

$$\partial_t \langle \rho_M \rangle + 3 \frac{\dot{\bar{a}}}{\bar{a}} \langle \rho_M \rangle = 0, \quad (4)$$

$$\partial_t \langle \rho_R \rangle + 4 \frac{\dot{\bar{a}}}{\bar{a}} \langle \rho_R \rangle = 0, \quad (5)$$

$$\partial_t (\bar{a}^6 \mathcal{Q}) + \bar{a}^4 \partial_t (\bar{a}^2 \langle \mathcal{R} \rangle) = 0, \quad (6)$$

where an overdot denotes a time derivative for volume-average observers “comoving” with the dust of density ρ_M . Here $\bar{a}(t) \equiv [\mathcal{V}(t)/\mathcal{V}(t_0)]^{1/3}$ is the volume-average scale factor, $\langle \mathcal{R} \rangle$ is the average spatial curvature scalar and

$$\mathcal{Q} = \frac{2}{3} (\langle \theta^2 \rangle - \langle \theta \rangle^2) - 2\langle \sigma^2 \rangle, \quad (7)$$

is the kinematic backreaction, which combines the variance in volume expansion and the shear scalar $\sigma^2 = \frac{1}{2}\sigma_{\alpha\beta}\sigma^{\alpha\beta}$. We use units in which $c = 1$. Equation (6) is a condition needed to ensure that (2) is the integral of (3). The integrability condition (6) constrains just one of the two unknowns \mathcal{Q} and $\langle \mathcal{R} \rangle$ in general. In the timescape model an ensemble of wall and void regions is further specified, thereby constraining $\langle \mathcal{R} \rangle$ and giving a coupled set of differential equations which can be solved.

The notion of “comoving with the dust” is reinterpreted in the timescape approach. Since particle geodesics cross during structure formation one must necessarily coarse-grain over scales larger than galaxies to define “dust” in cosmology. However, galaxies are not isolated particles whose masses remain invariant from last-scattering until today. In the timescape approach it is assumed that “dust” can only be defined as expanding fluid cells coarse-grained at a scale a few times larger than that of the largest typical nonlinear structures, so that the mass contained in a dust cell does not change on average. Given that the largest typical nonlinear structures are voids of diameter $30 h^{-1}\text{Mpc}$ [1, 2], we take the coarse-graining scale or *statistical homogeneity scale* to be comparable to the BAO scale, $100 h^{-1}\text{Mpc}$. The Buchert time parameter is therefore regarded as a collective coordinate of such a coarse-grained “dust” cell. Equations (2)–(6), which involve derivatives with respect to Buchert time, represent the evolution of a statistical geometry. The Buchert time parameter would only be directly measured by a *volume-average* isotropic observer, namely an observer who measures an isotropic CMB and whose local regional spatial curvature scalar happens to match the scalar curvature averaged over a horizon volume, $\langle \mathcal{R} \rangle$.

Following references [11, 12] we assume that the present epoch horizon volume, $\mathcal{V} = \mathcal{V}_i \bar{a}^3$, is a disjoint union of void and wall regions characterized by scale factors a_v and a_w related to the volume-average scale factor by

$$\bar{a}^3 = f_{vi} a_v^3 + f_{wi} a_w^3 \quad (8)$$

where f_{vi} and $f_{wi} = 1 - f_{vi}$ represent the fraction of the initial volume, \mathcal{V}_i , in void and wall regions respectively at an early unspecified epoch. The voids are assumed to have negative spatial curvature characterized by $\langle \mathcal{R} \rangle_v \equiv 6k_v/a_v^2$ with $k_v < 0$, while the wall regions [11] are on average spatially flat, $\langle \mathcal{R} \rangle_w = 0$.

In previous work the initial volume was assumed to be prescribed at the surface of last scattering. Furthermore, since finite infinity regions are only well-defined once gravitational collapse results in the formation of bound structures, the operational definition of f_{wi} and f_{vi} is complex. Following [11]–[13] we assume that f_{wi} is close to unity, consistent with the universe at last scattering being very close to a spatially flat FLRW model. The tiny void fraction $f_{vi} \ll 1$ then represents that fraction of the

present epoch horizon volume in which underdense perturbations were not compensated by overdense perturbations at last scattering. It is convenient to rewrite (8) as

$$f_v(t) + f_w(t) = 1, \quad (9)$$

where $f_w(t) = f_{wi}a_w^3/\bar{a}^3$ is the wall volume fraction and $f_v(t) = f_{vi}a_v^3/\bar{a}^3$ is the void volume fraction. Since $\langle\rho_M\rangle = \bar{\rho}_{M0}(\bar{a}/\bar{a}_0)^{-3}$ and $\langle\rho_R\rangle = \bar{\rho}_{R0}(\bar{a}/\bar{a}_0)^{-4}$, where the subscript zero refers to quantities evaluated at the present epoch, after solving (4) and (5) in the standard fashion the remaining independent Buchert equations in (2)–(6) may be written as

$$\frac{\dot{\bar{a}}^2}{\bar{a}^2} + \frac{\dot{f}_v^2}{9f_v(1-f_v)} - \frac{\alpha^2 f_v^{1/3}}{\bar{a}^2} = \frac{8\pi G}{3} \left(\bar{\rho}_{M0} \frac{\bar{a}_0^3}{\bar{a}^3} + \bar{\rho}_{R0} \frac{\bar{a}_0^4}{\bar{a}^4} \right), \quad (10)$$

$$\ddot{f}_v + \frac{\dot{f}_v^2(2f_v-1)}{2f_v(1-f_v)} + 3\frac{\dot{\bar{a}}}{\bar{a}}\dot{f}_v - \frac{3\alpha^2 f_v^{1/3}(1-f_v)}{2\bar{a}^2} = 0, \quad (11)$$

where $\alpha^2 \equiv -k_v f_{vi}^{2/3} > 0$. We note that (11) is unchanged from the corresponding equation in the matter only case [11, 12]. The acceleration equation (3) which may be derived from (10) and (11) is given by

$$\frac{\ddot{\bar{a}}}{\bar{a}} = \frac{2\dot{f}_v^2}{9f_v(1-f_v)} - \frac{4\pi G}{3} \frac{\bar{a}_0^3}{\bar{a}^3} \left[\bar{\rho}_{M0} + 2\bar{\rho}_{R0} \frac{\bar{a}_0}{\bar{a}} \right], \quad (12)$$

where we have made the substitutions [11]

$$\langle\mathcal{R}\rangle \equiv \frac{6k_v f_{vi}^{2/3} f_v^{1/3}}{\bar{a}^2}, \quad \mathcal{Q} \equiv \frac{2\dot{f}_v^2}{3f_v(1-f_v)}. \quad (13)$$

The first Buchert equation (10) is the equivalent of the Friedmann equation for the bare Hubble parameter, which from (8) is given by

$$\bar{H} \equiv \frac{\dot{\bar{a}}}{\bar{a}} = f_w H_w + f_v H_v, \quad (14)$$

where $H_w \equiv \dot{a}_w/a_w$ and $H_v \equiv \dot{a}_v/a_v$ are the Hubble parameters of the walls and voids respectively as determined by the clocks of volume-average observers. These satisfy an inequality

$$h_r \equiv H_w/H_v < 1. \quad (15)$$

It is an assumption of the timescape model that while any observer with a single clock will always determine wall regions to be expanding at a slower rate than void regions, the actual expansion rates depend on time parameters which differ on account of gravitational energy gradients between regions of different spatial curvature. In particular, observers in the denser (spatially flat) wall regions use the wall time parameter $d\tau_w = dt/\bar{\gamma}$, where

$$\bar{\gamma} = 1 + \left(\frac{1-h_r}{h_r} \right) f_v \quad (16)$$

is the *phenomenological lapse function* relating the clock of the wall observer to that of a volume-average observer.

Equation (10) is also conveniently written in the form

$$\bar{\Omega}_M + \bar{\Omega}_R + \bar{\Omega}_k + \bar{\Omega}_Q = 1, \quad (17)$$

where

$$\bar{\Omega}_M = \frac{8\pi G \bar{\rho}_{M0} \bar{a}_0^3}{3\bar{H}^2 \bar{a}^3}, \quad (18)$$

$$\bar{\Omega}_R = \frac{8\pi G \bar{\rho}_{R0} \bar{a}_0^4}{3\bar{H}^2 \bar{a}^4}, \quad (19)$$

$$\bar{\Omega}_k = \frac{\alpha^2 f_v^{1/3}}{\bar{a}^2 \bar{H}^2}, \quad (20)$$

$$\bar{\Omega}_Q = \frac{-\dot{f}_v^2}{9f_v(1-f_v)\bar{H}^2} = \frac{-(1-f_v)(1-\bar{\gamma})^2}{f_v\bar{\gamma}^2}, \quad (21)$$

are the volume-average or “bare” density parameters of matter, radiation, average spatial curvature and kinematic backreaction respectively. It would be straightforward to add a cosmological constant term to the right hand side of (10) with the addition of a further density parameter $\bar{\Omega}_\Lambda = \Lambda/(3\bar{H}^2)$, and in fact the equivalent solution with matter and a cosmological constant (but no radiation) has been derived in [22, 23]. Since we are investigating the possibility of a viable cosmology without dark energy, we set $\bar{\Omega}_\Lambda = 0$.

If we evaluate (17)–(21) at the present epoch we find that the present value of the phenomenological lapse parameter is given in terms of the other parameters by

$$\bar{\gamma}_0 = \frac{\sqrt{1-f_{v0}} \left(\sqrt{1-f_{v0}} + \sqrt{f_{v0}(1-f_{v0})(\bar{\Omega}_0 - 1)} \right)}{1 - f_{v0}\bar{\Omega}_0}, \quad (22)$$

where

$$\bar{\Omega}_0 \equiv \bar{\Omega}_{M0} + \bar{\Omega}_{R0} + \bar{\Omega}_{k0}, \quad (23)$$

which satisfies $1 < \bar{\Omega}_0 < f_{v0}^{-1}$. If we drop the subscript zero in (22) and (23) we obtain a generic relation for $\bar{\gamma}$ in terms of $\bar{\Omega}_M$, $\bar{\Omega}_R$ and $\bar{\Omega}_k$ at any epoch.

The bare cosmological parameters are not those determined by observers in galaxies in wall regions where the local spatially flat curvature is different to the volume-average one. Instead, using a matching procedure [11], the relevant dressed Hubble parameter is determined to be

$$H = \bar{\gamma}\bar{H} - \bar{\gamma}^{-1}\dot{\bar{\gamma}}. \quad (24)$$

The dressed matter density parameter $\Omega_M \equiv \bar{\gamma}^3\bar{\Omega}_M$ takes numerical values closer to the corresponding parameter for the concordance Λ CDM model when evaluated at the present epoch.

3. Solution for the two-scale model with radiation

In the case of purely nonrelativistic matter, $\rho_R = 0$, an analytic solution of the ODEs (10), (11) is readily found [12, 13]. This is in fact a consequence of the energy density scaling as a simple power of the total volume, as do the wall and void fractions. In the present case, which is not so simple, no further analytic integrals of the ODEs are easily obtained.

3.1. Early time series solution

Although an exact analytic solution to (10) and (11) is not to be found, a series solution in powers of $(\bar{H}_0 t)^{1/2}$ is readily obtained in the early time limit $t \rightarrow 0$. Here $\bar{H}_0 \equiv \bar{H}(t_0)$ is the bare Hubble constant. We find

$$\begin{aligned} \frac{\bar{a}}{\bar{a}_0} &= \sqrt{2} \bar{\Omega}_{R0}^{1/4} (\bar{H}_0 t)^{1/2} + \frac{\bar{\Omega}_{M0} (\bar{H}_0 t)}{3 \bar{\Omega}_{R0}^{1/2}} - \frac{7 \bar{\Omega}_{M0}^2 (\bar{H}_0 t)^{3/2}}{72 \sqrt{2} \bar{\Omega}_{R0}^{5/4}} \\ &+ \left(\frac{5 \bar{\Omega}_{M0}^3}{216 \bar{\Omega}_{R0}^{3/2}} + \frac{8 \bar{\alpha}^3}{5 \sqrt{5}} \right) \frac{(\bar{H}_0 t)^2}{\bar{\Omega}_{R0}^{1/2}} - \left(\frac{91 \bar{\Omega}_{M0}^3}{6912 \sqrt{2} \bar{\Omega}_{R0}^{3/2}} + \frac{7 \sqrt{2} \bar{\alpha}^3}{75 \sqrt{5}} \right) \frac{\bar{\Omega}_{M0} (\bar{H}_0 t)^{5/2}}{\bar{\Omega}_{R0}^{5/4}} \\ &+ \left(\frac{\bar{\Omega}_{M0}^3}{243 \bar{\Omega}_{R0}^{3/2}} + \frac{604 \bar{\alpha}^3}{8925 \sqrt{5}} \right) \frac{\bar{\Omega}_{M0}^2 (\bar{H}_0 t)^3}{\bar{\Omega}_{R0}^2} + \dots \end{aligned} \quad (25)$$

$$\begin{aligned} \frac{f_v}{\bar{\alpha}^3} &= \frac{2 \sqrt{2} (\bar{H}_0 t)^{3/2}}{5 \sqrt{5} \bar{\Omega}_{R0}^{3/4}} - \frac{8 \bar{\Omega}_{M0} (\bar{H}_0 t)^2}{25 \sqrt{5} \bar{\Omega}_{R0}^{3/2}} \\ &+ \frac{6617 \bar{\Omega}_{M0}^2 (\bar{H}_0 t)^{5/2}}{25500 \sqrt{10} \bar{\Omega}_{R0}^{9/4}} - \left(\frac{127 \sqrt{5} \bar{\Omega}_{M0}^3}{5967 \bar{\Omega}_{R0}^{3/2}} + \frac{576 \bar{\alpha}^3}{8125} \right) \frac{(\bar{H}_0 t)^3}{\bar{\Omega}_{R0}^{3/2}} \\ &+ \left(\frac{8811748927 \bar{\Omega}_{M0}^3}{100086480000 \sqrt{10} \bar{\Omega}_{R0}^{3/2}} + \frac{88522 \sqrt{2} \bar{\alpha}^3}{1503125} \right) \frac{\bar{\Omega}_{M0} (\bar{H}_0 t)^{7/2}}{\bar{\Omega}_{R0}^{9/4}} + \dots \end{aligned} \quad (26)$$

where $\bar{\alpha} \equiv \alpha / (\bar{a}_0 \bar{H}_0) = \bar{\Omega}_{k0}^{1/2} f_{v0}^{-1/6} \simeq 3 f_{v0}^{1/3} / (2 + f_{v0})$, which is a parameter close to unity, taking values in the range $0.973 < \bar{\alpha} < 0.999$ for solutions with $0.6 < f_{v0} < 0.9$. When $\alpha = 0$, then $f_v = 0$ and (25) reduces to the standard spatially flat FLRW solution for matter plus radiation, \bar{a}_{FLRW} . More generally we note that as $t \rightarrow 0$, then $f_v \rightarrow 0$ and the series solution (25) differs from the series solution for \bar{a}_{FLRW} at the level of terms $O(\bar{\alpha}^3 \bar{\Omega}_{R0}^{3/2} / \bar{\Omega}_{M0}^3) \ll 1$ and smaller in the coefficients of the powers $(\bar{H}_0 t)^n$, $n \geq 2$.

Using (25), (26) series solutions for all other relevant quantities can be obtained. For example, the void scale factor $a_v = \bar{a} f_v^{1/3} f_{vi}^{-1/3}$ takes the form

$$\frac{a_v}{a_{vi}} = \frac{2}{\sqrt{5}} (\bar{H}_0 t) + \frac{\sqrt{2} \bar{\Omega}_{M0}}{15 \sqrt{5} \bar{\Omega}_{R0}^{3/4}} (\bar{H}_0 t)^{3/2} - \frac{209 \bar{\Omega}_{M0}^2}{5100 \sqrt{5} \bar{\Omega}_{R0}^{3/2}} (\bar{H}_0 t)^2$$

$$\begin{aligned}
 & + \left(\frac{53621\sqrt{2}\bar{\Omega}_{\text{M0}}^3}{3978000\sqrt{5}\bar{\Omega}_{\text{R0}}^{3/2}} + \frac{8\sqrt{2}\bar{\alpha}^3}{1625} \right) \frac{(\bar{H}_0 t)^{5/2}}{\bar{\Omega}_{\text{R0}}^{3/4}} \\
 & + \left(\frac{261638807\bar{\Omega}_{\text{M0}}^3}{28149322500\sqrt{5}\bar{\Omega}_{\text{R0}}^{3/2}} + \frac{6716\bar{\alpha}^3}{901875\sqrt{5}} \right) \frac{\bar{\Omega}_{\text{M0}}\bar{\alpha}(\bar{H}_0 t)^3}{\bar{\Omega}_{\text{R0}}^{3/2}} + \dots
 \end{aligned} \tag{27}$$

where $a_{\text{vi}} \equiv f_{\text{vi}}^{-1/3}\bar{a}_0\bar{\alpha}$, which to leading order is linear in $\bar{H}_0 t$ as $t \rightarrow 0$, like a Milne universe, but differs at higher order. The wall scale factor $a_{\text{w}} = \bar{a}(1 - f_{\text{v}})^{1/3}f_{\text{vi}}^{-1/3}$ takes the form

$$\begin{aligned}
 \frac{a_{\text{w}}}{a_{\text{wi}}} & = \sqrt{2}\bar{\Omega}_{\text{R0}}^{1/4}(\bar{H}_0 t)^{1/2} + \frac{\bar{\Omega}_{\text{M0}}(\bar{H}_0 t)}{3\bar{\Omega}_{\text{R0}}^{1/2}} - \frac{7\bar{\Omega}_{\text{M0}}^2(\bar{H}_0 t)^{3/2}}{72\sqrt{2}\bar{\Omega}_{\text{R0}}^{5/4}} \\
 & + \left(\frac{5\bar{\Omega}_{\text{M0}}^3}{216\bar{\Omega}_{\text{R0}}^{3/2}} + \frac{4\bar{\alpha}^3}{75\sqrt{5}} \right) \frac{(\bar{H}_0 t)^2}{\bar{\Omega}_{\text{R0}}^{1/2}} - \left(\frac{91\bar{\Omega}_{\text{M0}}^3}{6912\sqrt{2}\bar{\Omega}_{\text{R0}}^{3/2}} + \frac{7\sqrt{2}\bar{\alpha}^3}{225\sqrt{5}} \right) \frac{\bar{\Omega}_{\text{M0}}(\bar{H}_0 t)^{5/2}}{\bar{\Omega}_{\text{R0}}^{5/4}} \\
 & + \left(\frac{\bar{\Omega}_{\text{M0}}^3}{243\bar{\Omega}_{\text{R0}}^{3/2}} + \frac{11927\bar{\alpha}^3}{401625\sqrt{5}} \right) \frac{\bar{\Omega}_{\text{M0}}^2(\bar{H}_0 t)^3}{\bar{\Omega}_{\text{R0}}^2} + \dots
 \end{aligned} \tag{28}$$

where $a_{\text{wi}} = f_{\text{wi}}^{-1/3}\bar{a}_0$, which is very close to the background solution (25), differing only at $\mathcal{O}[(\bar{H}_0 t)^2]$.

The relative expansion rate of walls and voids, and the phenomenological lapse function, are found to be

$$\begin{aligned}
 h_r & = \frac{1}{2} + \frac{3\bar{\Omega}_{\text{M0}}(\bar{H}_0 t)^{1/2}}{20\sqrt{2}\bar{\Omega}_{\text{R0}}^{3/4}} - \frac{463\bar{\Omega}_{\text{M0}}^2(\bar{H}_0 t)}{6800\bar{\Omega}_{\text{R0}}^{3/2}} + \left(\frac{332167\bar{\Omega}_{\text{M0}}^3}{5304000\sqrt{2}\bar{\Omega}_{\text{R0}}^{3/2}} + \frac{\bar{\alpha}^3}{65\sqrt{5}} \right) \frac{(\bar{H}_0 t)^{3/2}}{\bar{\Omega}_{\text{R0}}^{3/4}} \\
 & - \left(\frac{1452551123\bar{\Omega}_{\text{M0}}^3}{50043240000\bar{\Omega}_{\text{R0}}^{3/2}} + \frac{7329\bar{\alpha}^3}{120250\sqrt{5}} \right) \frac{\bar{\Omega}_{\text{M0}}(\bar{H}_0 t)^2}{\bar{\Omega}_{\text{R0}}^{3/2}} + \dots,
 \end{aligned} \tag{29}$$

$$\begin{aligned}
 \bar{\gamma} & = 1 + \frac{2\sqrt{2}\bar{\alpha}^3}{5\sqrt{5}\bar{\Omega}_{\text{R0}}^{3/4}}(\bar{H}_0 t)^{3/2} - \frac{14\bar{\Omega}_{\text{M0}}\bar{\alpha}^3}{25\sqrt{5}\bar{\Omega}_{\text{R0}}^{3/2}}(\bar{H}_0 t)^2 + \frac{3781\bar{\Omega}_{\text{M0}}^2\bar{\alpha}^3}{5100\sqrt{10}\bar{\Omega}_{\text{R0}}^{9/4}}(\bar{H}_0 t)^{5/2} \\
 & - \left(\frac{142189\bar{\Omega}_{\text{M0}}^3}{298350\sqrt{5}\bar{\Omega}_{\text{R0}}^{3/2}} + \frac{736\bar{\alpha}^3}{8125} \right) \frac{\bar{\alpha}^3(\bar{H}_0 t)^3}{\bar{\Omega}_{\text{R0}}^{3/2}} + \dots
 \end{aligned} \tag{30}$$

In [11] the matter-only solution was joined to the spatially flat FLRW solution with matter and radiation, which corresponds to the $\bar{\alpha} = 0$ limit above. We see that all the assumptions made in the matching procedure were correct, with one exception. In [11] it was assumed that as $t \rightarrow 0$ we would have $h_r \rightarrow 1$, whereas it turns out that $h_r \rightarrow \frac{1}{2}$. Actually, this small difference in assumptions makes no difference to any of the physical conclusions derived in [11], since the late time solution quickly reaches a tracking limit which is largely independent of the initial conditions. Furthermore, in deriving constraints from the early universe, such as primordial nucleosynthesis bounds,

calculations in [11] only required the property that $\bar{\gamma} \rightarrow 1$ and $f_v \rightarrow 0$ as $t \rightarrow 0$, which remains correct in the full solution with radiation. The exact dependence of h_r as $t \rightarrow 0$ may be of relevance for determination of features of the matter power spectrum. However, such features remain to be determined.

It is possible to invert the series (25) to obtain an expression for $\bar{H}_0 t$ in terms of a series in \bar{a}/\bar{a}_0 at very early times. This enables one to determine the epoch of matter–radiation equality, for example, when $\bar{a}_{\text{eq}}/\bar{a}_0 = \bar{\Omega}_{R0}/\bar{\Omega}_{M0}$. It turns out that the terms in \bar{a} introduce differences of less than 0.1% from the leading order spatially flat FLRW result, ‡ $\bar{H}_0 t_{\text{eq}} = 2(2 - \sqrt{2})\bar{\Omega}_{R0}^{3/2}/(3\bar{\Omega}_{M0}^2)$.

3.2. Numerical solutions and results

We have determined further terms in the series expansions (25), (26) and have established that they provide accurate solutions well beyond the epoch of recombination, when compared to numerical solutions. For practical investigations, however, it is convenient to use the series expansions to provide initial conditions at an early time, and to integrate the ODEs (10) and (11) numerically. We begin integrations after the epoch of nucleosynthesis when the universe is radiation dominated but the number of relativistic species is no longer affected by phase transitions, e.g., at $\bar{H}_0 t \simeq 5 \times 10^{-11}$ when the universe is about a year old.

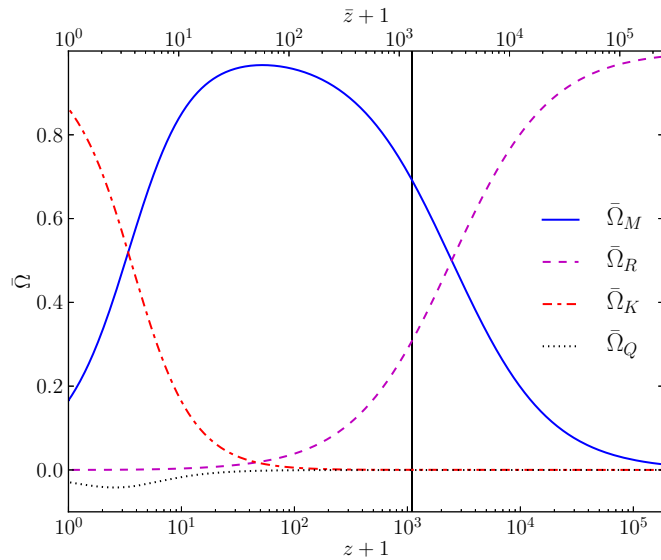


Figure 1. Bare density parameters (18)–(21) for the full numerical solution, as a function of $z+1 = \bar{\gamma}\bar{a}_0/(\bar{\gamma}_0\bar{a})$, for the dressed parameters $H_0 = 61.7 \text{ km sec}^{-1} \text{ Mpc}^{-1}$, $\Omega_{M0} = 0.410$. (The redshift, z , is the dressed parameter measured by wall observers, and \bar{z} is the bare redshift.) The vertical bar at $1094.88 < z < 1100.46$ represents the width of the uncertainty in the redshift of decoupling for our chosen range of $\eta_{B\gamma}$.

‡ Here \bar{H}_0 is, however, the bare Hubble constant which differs from the dressed Hubble constant, H_0 , according to $H_0 = (4f_{v0}^2 + 4f_{v0} + 4)\bar{H}_0/[2(2 + f_{v0})]$ [12, 13].

In figure 1 we display the variation of the bare density parameters as a function of redshift for one choice of (H_0, Ω_{M0}) values which fit cosmological data well. For redshifts $z \lesssim 10$ the bare density parameters are essentially indistinguishable from those computed for the matter-only solution [11]–[13]. The full matter plus radiation solution is certainly required to make reliable estimates of $\bar{\Omega}_M$ and $\bar{\Omega}_R$ at redshifts larger than that corresponding to the maximum of $\bar{\Omega}_M$, i.e., at $z \gtrsim 50$.

In earlier work we joined the matter-dominated solution [12] to a spatially flat FLRW with matter plus radiation at the surface of last scattering [11, 14, 15]. This allowed a rough estimate of the angular diameter distance of the sound horizon, and of the effective comoving BAO scale which is independently measured in galaxy clustering statistics. Since the approximations were rough we simply took $z_{\text{dec}} \simeq 1100$ as an estimate of the epoch of photon decoupling, $\theta_* \simeq 0.01$ rad as an estimate of the angular acoustic scale, and $104 h^{-1} \text{Mpc}$ as an estimate of the effective comoving BAO scale based on measurements for the standard cosmology known at the time [11, 14].

Given a full numerical solution including radiation, we can determine both the epoch of photon decoupling and the subsequent baryon drag epoch directly in parallel to our numerical integrations, using the standard physics of the recombination era adapted to the timescape model, as discussed in Appendix B. The volume-average sound horizon scale at any epoch is given by

$$\bar{D}_s = \frac{\bar{a}(t)}{\bar{a}_0} \frac{c}{\sqrt{3}} \int_0^{\bar{x}_{\text{dec}}} \frac{d\bar{x}}{\bar{x}^2 \bar{H} \sqrt{1 + 0.75 \bar{x} \bar{\Omega}_{B0} / \bar{\Omega}_{\gamma 0}}}, \quad (31)$$

where $\bar{\Omega}_{\gamma 0} = 2g_*^{-1} \bar{\Omega}_{R0}$ is the volume-average photon density parameter at the present epoch and $g_* = 3.36$ is the relative degeneracy factor of relativistic species. We fix the value of $\bar{\Omega}_{B0} = \eta_{B\gamma} m_p \bar{n}_{\gamma 0}$ in terms of the proton mass, m_p , the present epoch volume-average photon density, $\bar{n}_{\gamma 0}$, and the baryon-to-photon ratio, $\eta_{B\gamma}$. For BAO measurements, the relevant comoving size of the sound horizon is that at the baryon drag epoch, which occurs when $c\tau_d \simeq 1$, where τ_d is the drag depth (B.12).

Examples of the estimation of the decoupling redshift, z_{dec} , from the peak of the visibility function are shown in figure 2 for fixed values of (H_0, Ω_{M0}) , with three different values of the baryon-to-photon ratio, giving rise to different values of $\bar{\Omega}_{B0}$ (or of $\Omega_{B0} = \bar{\gamma}_0^3 \bar{\Omega}_{B0}$). It is a feature of the timescape model that for a given baryon-to-photon ratio, the baryon fraction at decoupling is increased relative to the standard Λ CDM model. Thus it is possible to match features of the acoustic peaks [11] for baryon-to-photon ratios for which there is no primordial lithium abundance anomaly [24]. In keeping with past work [11, 14], we perform calculations for the range $\eta_{B\gamma} = (5.1 \pm 0.5) \times 10^{-10}$ on the basis of constraints from light element abundances alone§ [25, 26].

§ A higher value is assumed in the Λ CDM fits of CMB data, giving rise to the lithium abundance anomaly. While there is an intrinsic tension in the light element data between abundances of deuterium and lithium-7 [26], for the range of $\eta_{B\gamma}$ we adopt here, all abundances fall within 2σ .

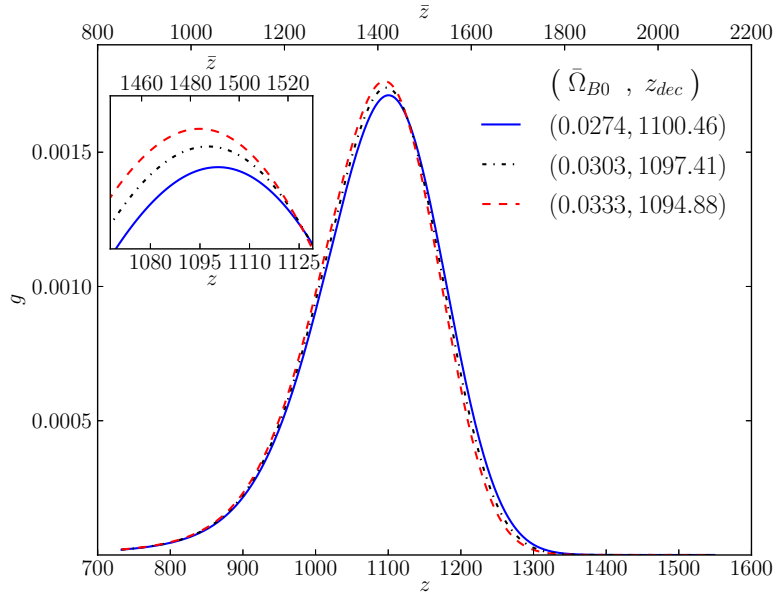


Figure 2. The visibility function (B.10) is plotted as a function of the dressed redshift, z , (and also of \bar{z}). For this example, $H_0 = 61.7 \text{ km sec}^{-1} \text{ Mpc}^{-1}$ (or $\bar{H}_0 = 50.1 \text{ km sec}^{-1} \text{ Mpc}^{-1}$), $\Omega_{\text{M}0} = 0.410$ (or $\bar{\Omega}_{\text{M}0} = 0.167$), with three different values of the baryon-to-photon ratio: $10^{10}\eta_{B\gamma} = \{4.6, 5.1, 5.6\}$ (which correspond to $\bar{\Omega}_{\text{B}0} = \{0.0274, 0.0303, 0.0333\}$ respectively).

Using the procedures discussed in Appendix A we have conducted numerical integrations over the parameter space to investigate the extent to which the timescape model parameters can be constrained using recent Planck data [27]. We see from (A.1)–(A.3) that since the curvature parameter $\bar{\alpha}$ can be absorbed into a rescaling of the time variable there are effectively three independent parameters, \bar{H} , $\alpha_{\text{M}0}$ and $\alpha_{\text{R}0}$, or equivalently \bar{H}_0 , $\bar{\Omega}_{\text{M}0}$ and $\bar{\Omega}_{\text{R}0}$. Since the bare radiation density parameter is constrained by measurements of the CMB temperature, this leaves two independent parameters of interest. We can take these to be either the bare parameters, \bar{H}_0 and $\bar{\Omega}_{\text{M}0}$, or equivalently the dressed Hubble constant, $H_0 = \bar{\gamma}_0 \bar{H}_0 - \bar{\gamma}_0^{-1} \dot{\bar{\gamma}}|_0$, and the dressed matter density parameter $\Omega_{\text{M}0} = \bar{\gamma}_0^3 \bar{\Omega}_{\text{M}0}$. For the figures below we will use the dressed parameters, since H_0 ideally corresponds to our measured average Hubble constant, while $\Omega_{\text{M}0}$ is numerically closer to that of the homogeneous Λ CDM cosmology.

In figure 3 and figure 4 we display contours of the decoupling redshift, z_{dec} , and the baryon drag redshift, z_{drag} , for the case of a fixed $\eta_{B\gamma} = 5.1 \times 10^{-10}$, but with the two independent parameters (H_0 , $\Omega_{\text{M}0}$) varying. In each case we display the dressed redshifts determined by wall observers such as ourselves.

In figure 5 we display two sets of contours in the (H_0 , $\Omega_{\text{M}0}$) parameter space: firstly, parameters which match the acoustic scale of the sound horizon $\theta_* = 0.0104139$ determined from the Planck satellite data [27] to within $\pm 2\%$, $\pm 4\%$ or $\pm 6\%$; and secondly parameters which similarly match the present effective comoving scale of the

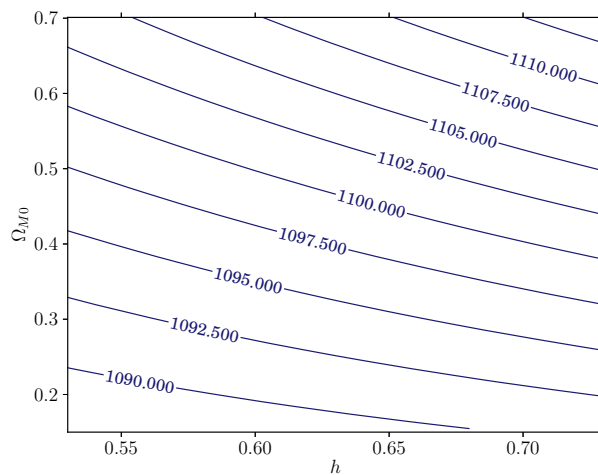


Figure 3. Contours of decoupling redshift, z_{dec} , in the space of dressed parameters (h , $\Omega_{\text{M}0}$), (where $H_0 = 100 h \text{ Mpc}$). Contours are shown for the case $\eta_{B\gamma} = 5.1 \times 10^{-10}$.

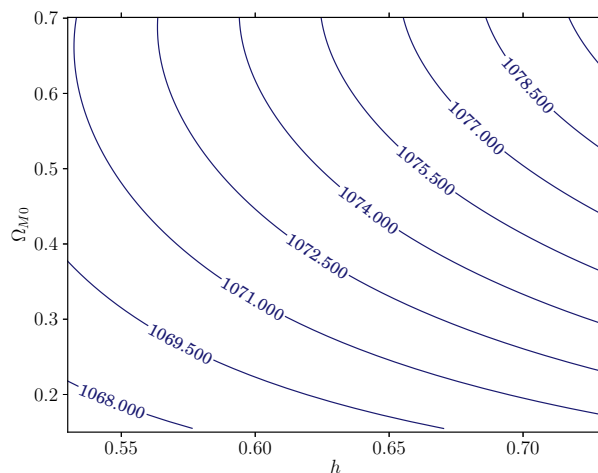


Figure 4. Contours of the redshift of the baryon drag epoch, z_{drag} , in the space of dressed parameters (h , $\Omega_{\text{M}0}$), (where $H_0 = 100 h \text{ Mpc}$). Contours are shown for the case $\eta_{B\gamma} = 5.1 \times 10^{-10}$.

sound horizon at baryon drag epoch as determined by the standard Λ CDM model analysis of the Planck data, namely $\| 98.88 h^{-1} \text{ Mpc}$ [27]. This figure updates figure 4 of [15] both in terms of using the latest data [27], and also in using our new full matter–radiation solution to determine the relevant scales.

The constraints obtained from figure 5 are not statistical constraints of the sort

$\|$ Since the Hubble constant $H_0 = 67.11 \text{ km sec}^{-1} \text{ Mpc}^{-1}$ determined from the Planck satellite is a fit to the Λ CDM model, any effective present comoving scale must be given in units $h^{-1} \text{ Mpc}$, as the timescape model will generally yield a different value for H_0 . In all cases, we use the values determined from the Planck data only.

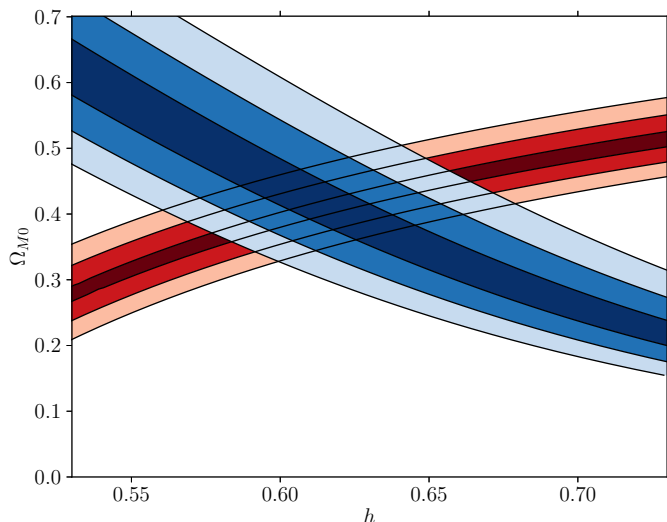


Figure 5. Contours of (h, Ω_{M0}) parameter values for which the angular diameter of the sound horizon at decoupling matches the angular scale $\theta_* = 0.0104139$ [27] to within $\pm 2\%$, $\pm 4\%$ and $\pm 6\%$ are shown in blue (upper left to lower right). Contours of parameter values for which the present-day effective comoving scale of the sound horizon at the baryon drag epoch matches the value $98.88 h^{-1} \text{Mpc}$ [27] are shown in red (lower left to upper right). In each case the baryon-to-photon ratio is assumed to be in the range $4.6 < 10^{10} \eta_{B\gamma} < 5.6$.

that could be obtained by fully fitting the Planck data directly to the timescape model. However, the angular scale in particular is unlikely to differ much from that of the FLRW model analysis, and the 2% constraint is a reasonable estimate of uncertainty. There is greater uncertainty in the determination of the BAO scale since the timescape model involves a potential recalibration of the relative proportions of baryonic and nonbaryonic dark matter which needs to be accounted for in fitting the acoustic peaks in CMB anisotropy data[¶].

If we nonetheless take the 2% constraint on θ_* and the 6% constraint on r_{drag} as estimates of the uncertainty, then this corresponds to the constraints $H_0 = 61.7 \pm 3.0 \text{ km sec}^{-1} \text{ Mpc}^{-1}$, $\Omega_{M0} = 0.41_{-0.06}^{+0.05}$. Constraints on other parameters with these bounds are given in table 1. It is interesting to note that the constraints on (H_0, Ω_{M0}) are well in agreement⁺ with the constraints obtained from the analysis of 272 SDSS-II supernova distances [28] in the timescape cosmology, as shown in the second panel of figure 8 of [15]. The timescape model therefore remains competitive.

Even if the constraints on r_{drag} were to change in a detailed fit of the acoustic

[¶] The ratio of the nonbaryonic cold dark matter density to the baryonic density found for the Λ CDM model with the Planck data [27], $\Omega_{C0}/\Omega_{B0} = 5.4 \pm 0.2$, is well within the range found for the timescape model in table 1, which justifies the approach we have taken.

⁺ For supernova analysis constraints on H_0 are subject to an overall normalization of the distance scale. In the present case, using the normalization chosen by the authors of [28] the constraints on both H_0 and Ω_{M0} from supernovae [15] coincide with parameters which fit the Planck data, as given in table 1.

Table 1. Constraints on the cosmological parameters of the timescape model obtained from a $\pm 2\%$ match to the angular scale, θ_* , of the sound horizon at decoupling; and to a $\pm 6\%$ match to the effective comoving scale, r_{drag} , of the sound horizon at the baryon drag epoch, using recent values from the Planck satellite analysis [27].

Parameter		Range
Dressed Hubble constant	H_0	$61.7 \pm 3.0 \text{ km}/(\text{sec} \cdot \text{Mpc})$
Dressed matter density parameter	$\Omega_{\text{M}0}$	$0.41^{+0.06}_{-0.05}$
Dressed baryon density parameter	$\Omega_{\text{B}0}$	$0.074^{+0.013}_{-0.011}$
Age of universe (galaxy/wall observer)	$\tau_{\text{w}0}$	$14.2 \pm 0.5 \text{ Gyr}$
Apparent acceleration onset redshift	z_{acc}	$0.46^{+0.26}_{-0.25}$
Present void fraction	$f_{\text{v}0}$	$0.695^{+0.041}_{-0.051}$
Present phenomenological lapse function	$\bar{\gamma}_0$	$1.348^{+0.021}_{-0.025}$
Bare Hubble constant	\bar{H}_0	$50.1 \pm 1.7 \text{ km}/(\text{sec} \cdot \text{Mpc})$
Bare matter density parameter	$\bar{\Omega}_{\text{M}0}$	$0.167^{+0.036}_{-0.037}$
Bare baryon density parameter	$\bar{\Omega}_{\text{B}0}$	$0.030^{+0.007}_{-0.005}$
Bare radiation density parameter	$\bar{\Omega}_{\text{R}0}$	$(5.00^{+0.56}_{-0.48}) \times 10^{-5}$
Bare curvature parameter	$\bar{\Omega}_{\text{k}0}$	$0.862^{+0.024}_{-0.032}$
Bare backreaction parameter	$\bar{\Omega}_{\text{Q}0}$	$-0.0293^{+0.0033}_{-0.0036}$
Nonbaryonic/baryonic matter densities ratio	$\bar{\Omega}_{\text{C}0}/\bar{\Omega}_{\text{B}0}$	$4.6^{+2.5}_{-2.1}$
Age of universe (volume-average observer)	t_0	$17.5 \pm 0.6 \text{ Gyr}$

peaks to the timescape model, we can at least rule out parameters by determining the ratio of matter to radiation densities at the epoch of photon decoupling. In figure 6 we display contours of the $\bar{\Omega}_M/\bar{\Omega}_R$ ratio at z_{dec} . While there is no direct constraint on the degree to which $\bar{\Omega}_M/\bar{\Omega}_R$ can differ from that of the concordance Λ CDM cosmology, it is certainly the case that matter–radiation equality has to occur well before decoupling in order that the standard physics of recombination applies. In this manner we can rule out parameters $\Omega_{\text{M}0} < 0.2$ if $H_0 < 65 \text{ km sec}^{-1} \text{ Mpc}^{-1}$. For the parameters of table 1, the ratio $\bar{\Omega}_M/\bar{\Omega}_R \simeq 2$ at decoupling, which differs from the ratio $\bar{\Omega}_M/\bar{\Omega}_R \simeq 3$ for the concordance Λ CDM model.

As compared to earlier best-fit values [14], the best-fit age of the universe with the new constraints, $\tau_{\text{w}0} = 14.2 \pm 0.5 \text{ Gyr}$, is somewhat closer to the Λ CDM concordance cosmology value.

4. Conclusion

In this paper we have derived solutions to the Buchert equations [17, 18] with matter and a radiation fluid. The solutions smoothly interpolate between a very early epoch, in which the relevant physics was that of the standard hot big bang with an almost homogeneous FLRW background, and a late time universe in which the average evolution is not that of a FLRW model even though a statistical notion of homogeneity persists

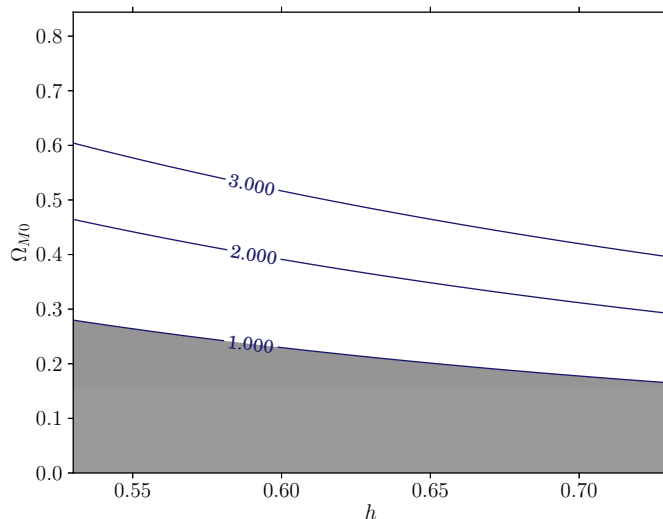


Figure 6. Contours of $\bar{\Omega}_M/\bar{\Omega}_R$ at z_{dec} , in the space of dressed parameters (h, Ω_{M0}) , (where $H_0 = 100 h \text{ Mpc}$). The shaded region with $\bar{\Omega}_M/\bar{\Omega}_R < 1$ is certainly ruled out.

when one averages on $\gtrsim 100 h^{-1}\text{Mpc}$ scales. Both the early time series solutions (25), (26) and the full numerical integrations can produce solutions of the Buchert equations for a late-time ensemble of spatially flat wall regions and negatively curved void regions irrespective of the observational interpretation. Our specific calibration of parameters is that relevant to the timescape cosmology [11]–[13] in which the Buchert time parameter for the statistical volume-average geometry is assumed to differ from that of observers in bound structures, on account of gravitational energy gradients which become significant once nonlinear structures such as voids dominate average cosmic evolution.

The timescape cosmology is phenomenologically successful, to the extent that it has been tested, and further tests require that its methodology is developed in detail. This paper takes key steps towards a full analysis of the acoustic peaks in the CMB anisotropy spectrum. The new solutions have enabled us to directly determine the epochs of photon–electron decoupling, z_{dec} , and of photon–baryon Compton scattering decoupling, z_{drag} , and consequently the scale of the sound horizon at these epochs.

With these refinements the parameters of table 1 which agree with both the acoustic scale, θ_* , and the BAO scale, r_{drag} , from the Planck data [27] remain in concordance with the outcome [15] of the fit of 277 supernovae distances from the SDSS-II survey [28]. Furthermore, this agreement is obtained for values of the baryon–to–photon ratio, $\eta_{B\gamma}$, for which the primordial lithium-7 abundance is not anomalous. The timescape model therefore remains a viable competitor to the standard cosmology.

A detailed treatment of the acoustic peaks in the CMB data may of course still challenge the timescape cosmology, as it will certainly further tighten the constraints. Work on this problem, which requires a revisiting of CMB data analysis from first principles, is in progress. As shown in figure 6, the new results in the present paper already allow us to rule out portions of the parameter space, such as $\bar{\Omega}_{M0} < 0.2$ if

$H_0 < 65 \text{ km sec}^{-1} \text{ Mpc}^{-1}$, which were still admissible in previous studies [14, 15]. Interestingly, the tightening of constraints in the present paper has also pushed the value of the age of the universe (in wall time) closer to that of the Λ CDM cosmology.

It should be stressed that the value of the average Hubble constant, $H_0 = 61.7 \pm 3.0 \text{ km sec}^{-1} \text{ Mpc}^{-1}$, inferred above* is a model-dependent fit to the timescape cosmology in the same way that the value quoted by the Planck satellite team, namely $67.4 \pm 1.4 \text{ km sec}^{-1} \text{ Mpc}^{-1}$ [27], is a model-dependent fit to the FLRW cosmology. There has been much interest about the apparent discrepancy between this Λ CDM model value of H_0 determined from the Planck satellite and the somewhat larger values from local measurements [29]. In the timescape model, a larger value of the Hubble parameter is expected below the scale of statistical homogeneity‡, and this may impact the calibration of the distance scale. Such issues are further discussed in a separate paper [30]. While no single piece of evidence provides conclusive proof of the timescape model, a number of recent observations which are puzzles for the standard cosmology – the primordial lithium-7 abundance; the local versus global values of H_0 ; a possible nonkinematic component to the CMB dipole [30, 31] – are consistent with expectations of the timescape cosmology. The results of the present paper provide a further stepping stone to even more detailed tests of the timescape scenario.

Acknowledgments

This work was supported by the Marsden Fund of the Royal Society of New Zealand. We thank Teppo Mattsson, Peter Smale and Nezihe Uzun for discussions.

Appendix A. Numerical integration

For the purposes of numerical integration it is convenient to write the derivatives with respect to $x \equiv \bar{a}/\bar{a}_0$, yielding the system of three coupled ODEs

$$\frac{dt'}{dx} = \frac{x\sqrt{1+x^2F^2}}{\sqrt{f_v^{1/3}x^2 + \alpha_{M0}x + \alpha_{R0}}}, \quad (\text{A.1})$$

$$\frac{df_v}{dx} = 3F\sqrt{f_v(1-f_v)}, \quad (\text{A.2})$$

$$\frac{dF}{dx} = \frac{(1+x^2F^2) \left[f_v^{-1/6} \sqrt{1-f_v} + F(\alpha_{M0} + 2\alpha_{R0}x^{-1}) \right]}{2 \left(f_v^{1/3}x^2 + \alpha_{M0}x + \alpha_{R0} \right)} - F \left(\frac{3}{x} + 2xF^2 \right), \quad (\text{A.3})$$

* For the timescape model this uncertainty is not yet statistical, as discussed above. Statistical uncertainties obtained from a detailed analysis of the Doppler peaks are likely to be of the same order as those quoted by the Planck team for the Λ CDM model [27].

‡ For the parameter values of table 1 the maximum value of the Hubble constant measured locally by a wall/galaxy observer to the other side of a void below the statistical homogeneity scale is $\frac{3}{2}\bar{H}_0 = 75.2^{+2.0}_{-2.6} \text{ km sec}^{-1} \text{ Mpc}^{-1}$.

in the dimensionless variables $t' \equiv \bar{\alpha}\bar{H}_0 t$, f_v and $F \equiv \partial_x f_v / [3\sqrt{f_v(1-f_v)}]$, where $\alpha_{M0} \equiv \bar{\alpha}^{-2}\bar{\Omega}_{M0}$ and $\alpha_{R0} \equiv \bar{\alpha}^{-2}\bar{\Omega}_{R0}$. The wall time parameter, $\tau_w = \int \bar{\gamma}^{-1} dt$, may be determined also by integrating the equation

$$\bar{\alpha}\bar{H}_0 \frac{d\tau_w}{dx} = \frac{1 - f_v(1 + x^2 F^2)}{1 - f_v + xF\sqrt{f_v(1-f_v)}} \frac{dt'}{dx}. \quad (\text{A.4})$$

Given an initial estimate of f_{v0} , the tracker solution [12, 13] is used to estimate $\bar{\Omega}_{M0} \simeq 4(1 - f_{v0})/(2 + f_{v0})^2$, $\bar{\Omega}_{k0} \simeq 9f_{v0}/(2 + f_{v0})^2$, $\bar{\alpha}^2 \simeq 9f_{v0}^{2/3}/(2 + f_{v0})^2$ and $\alpha_{M0} = 4(1 - f_{v0})/[9f_{v0}^{2/3}]$. Since $\bar{\Omega}_{R0} = \kappa g_* T_0^4 / (\bar{H}_0^2 \bar{\gamma}_0^4)$, where $\kappa \equiv 4\pi^3 G k_B^4 / (45\hbar^3 c^5)$, $g_* = 3.36$ and $T_0 = 2.725$ K, then given a value of \bar{H}_0 and the tracker solution estimates for $\bar{\Omega}_{M0}$ and $\bar{\Omega}_{k0}$ we can solve (22) to estimate $\bar{\gamma}_0$, $\bar{\Omega}_{R0}$ and α_{R0} .

Initial values of the variables are now determined at an early initial time using the series solutions (25), (26), or the equivalent series in x :

$$\begin{aligned} \bar{H}_0 \bar{\alpha} t = & \frac{x^2}{2\alpha_{R0}^{1/2}} - \frac{\alpha_{M0} x^3}{6\alpha_{R0}^{3/2}} + \frac{3\alpha_{M0}^2 x^4}{32\alpha_{R0}^{5/2}} - \left(\frac{2\sqrt{5}}{125\alpha_{R0}^2} + \frac{\alpha_{M0}^3}{16\alpha_{R0}^{7/2}} \right) x^5 \\ & + \left(\frac{7\sqrt{5}\alpha_{M0}}{300\alpha_{R0}^3} + \frac{35\alpha_{M0}^4}{768\alpha_{R0}^{9/2}} \right) x^6 - \left(\frac{402\sqrt{5}\alpha_{M0}^2}{14875\alpha_{R0}^4} + \frac{9\alpha_{M0}^5}{256\alpha_{R0}^{11/2}} \right) x^7 + \dots \end{aligned} \quad (\text{A.5})$$

$$\begin{aligned} f_v = & \frac{\sqrt{5}x^3}{25\alpha_{R0}^{3/2}} - \frac{9\sqrt{5}\alpha_{M0}x^4}{250\alpha_{R0}^{5/2}} + \frac{639\sqrt{5}\alpha_{M0}^2 x^5}{21250\alpha_{R0}^{7/2}} - \left(\frac{6}{325\alpha_{R0}^3} + \frac{5553\sqrt{5}\alpha_{M0}^3}{221000\alpha_{R0}^{9/2}} \right) x^6 \\ & + \left(\frac{11106\alpha_{M0}}{300625\alpha_{R0}^4} + \frac{295461027\sqrt{5}\alpha_{M0}^4}{13900900000\alpha_{R0}^{11/2}} \right) x^7 + \dots \end{aligned} \quad (\text{A.6})$$

We then integrate the ODEs (A.1)–(A.4) until the present epoch is reached at $x_0 = 1$, giving the exact numerical values $t'_0 = \bar{\alpha}\bar{H}_0 t_0$, f_{v0} , F_0 and $\bar{\alpha}\bar{H}_0 \tau_{w0}$. We also have $\bar{\gamma}_0 = [1 - f_{v0} + F_0\sqrt{f_{v0}(1-f_{v0})}] / [1 - f_{v0}(1 + F_0^2)]$.

Only two parameters, α_{M0} and α_{R0} , appear in the ODEs (A.1)–(A.3). Solutions with fixed α_{M0} , α_{R0} therefore represent a class of solutions which are physically equivalent under a rescaling of the parameters $\bar{\alpha}$, $\bar{\Omega}_{M0}$ and $\bar{\Omega}_{R0}$, while keeping the ratio $\bar{\Omega}_{M0}/\bar{\Omega}_{R0}$ fixed. A general solution does not have $\bar{H} = \bar{H}_0$ at $x_0 = 1$; to impose this condition we identify the right hand side of (A.1) at $x_0 = 1$ with $\bar{\alpha}$, from which precise values of $\bar{\Omega}_{M0} = \bar{\alpha}^2\alpha_{M0}$, $\bar{\Omega}_{R0} = \bar{\alpha}^2\alpha_{R0}$ and $\bar{H}_0 t_0$ may be determined.

Appendix B. Recombination and baryon drag epoch

In [11] the epoch of photon decoupling was set by the rough condition consistent with the Saha equation that $z_{\text{dec}} + 1 \simeq 1100$ as measured by a wall observer, or equivalently $x_{\text{dec}} = \bar{z}_{\text{dec}} + 1 = \bar{\gamma}_0(1 + z_{\text{dec}})/\bar{\gamma}_{\text{dec}}$, giving $x_{\text{dec}} \simeq 1518$ if $\bar{\gamma}_0 = 1.38$, given that $\bar{\gamma}_{\text{dec}} \simeq 1$.

In the present paper, we determine the epoch of photon decoupling more precisely, using the standard physics of recombination as described, for example, by Weinberg [32]. Since the universe is very close to that of the standard FLRW model at this epoch there is no difference in any physical processes, but merely in the calibration of parameters

relative to their present epoch values using the background solution. In particular, it is convenient to work with the volume-average parameters that appear in the Buchert equations, and therefore to work with the CMB photon temperature, \bar{T} , as measured by a volume-average observer. In the very early universe this is indistinguishable from the CMB photon temperature, T , measured by a wall observer. However, in general the two temperatures are related by

$$\bar{T} = \bar{\gamma}^{-1} T, \quad (\text{B.1})$$

giving a significant difference at the present epoch.

Following helium recombination, the ionization fraction of hydrogen is given by $X \equiv \bar{n}_p/\bar{n}$, where

$$\bar{n} = \bar{n}_p + \bar{n}_H = 0.76 \bar{n}_B \quad (\text{B.2})$$

is the combined number density of ionized and atomic hydrogen. The relation to the baryon number density, \bar{n}_B , arises from assuming that helium makes up 24% of baryons in weight. In our case, the bare baryon number density is given by

$$\bar{n}_B = \frac{3\bar{H}_0^2 \bar{\Omega}_{B0}}{8\pi G m_p} \left(\frac{\bar{T}}{\bar{T}_{\gamma 0}} \right)^3, \quad (\text{B.3})$$

where $\bar{\Omega}_{B0}$ is the present epoch bare baryon matter density parameter, $\bar{T}_{\gamma 0} = \bar{\gamma}_0^{-1} 2.275 \text{ K}$ and m_p the proton mass.

The ionization fraction is determined by solving the Peebles equation [33]

$$\frac{dX(t)}{dt} = \left(\frac{\Gamma_{2s} + 3P\Gamma_{2p}}{\Gamma_{2s} + 3P\Gamma_{2p} + \beta} \right) [-X^2 + S^{-1}(1 - X)] \mathcal{A} \bar{n}, \quad (\text{B.4})$$

where $\mathcal{A}(\bar{T})$ is the effective recombination rate to the excited $2s$ and $2p$ states; $\Gamma_{2s} = 8.22458 \text{ s}^{-1}$ and $\Gamma_{2p} = 4.699 \times 10^8 \text{ s}^{-1}$ are decay rates from the $2s$ and $2p$ states;

$$\beta = \left(\frac{m_e k_B \bar{T}}{2\pi \hbar^2} \right)^{3/2} \exp(-B_2/k_B \bar{T}) \mathcal{A} \quad (\text{B.5})$$

is the ionization rate from the excited states;

$$P = \frac{8\pi \bar{H}}{3\lambda_\alpha^3 \Gamma_{2p} \bar{n}_{1s}} \quad (\text{B.6})$$

is the photon survival probability, with $\lambda_\alpha = 1215.682 \times 10^{-8} \text{ cm}$ and $\bar{n}_{1s} \simeq \bar{n}_H$;

$$S \equiv 0.76 \bar{n}_B \left(\frac{m_e k_B \bar{T}}{2\pi \hbar^2} \right)^{-3/2} \exp(B_1/k_B \bar{T}); \quad (\text{B.7})$$

and $B_n = m_e e^4 / (2\hbar^2 n^2) = 13.6 n^{-2} \text{ eV}$ is the binding energy of the state with principal quantum number n . Detailed numerical calculations of $\mathcal{A}(\bar{T})$ can be fit by the formula [32, 34]

$$\mathcal{A} = \frac{1.4337 \times 10^{-10} \bar{T}^{-0.6166} \text{ cm}^3 \text{ s}^{-1}}{1 + 5.085 \times 10^{-3} \bar{T}^{0.5300}}, \quad (\text{B.8})$$

where \bar{T} is given in degrees Kelvin. The Saha equation

$$X(1 + SX) = 1 \quad (\text{B.9})$$

is an excellent approximation for the ionization fraction when X is close to unity during the initial equilibrium. It may therefore be used to provide an initial value for the differential equation (B.4) at $\bar{T} = 4226$ K, or $z = 1550$ after the end of helium recombination. For practical purposes, the differential equation (B.4) can be rewritten as an ODE in \bar{T} using $dt = -d\bar{T}/(\bar{H}\bar{T})$ or as an ODE in x using (A.1) divided by $\bar{\alpha}$.

The *visibility function*,

$$g(t) \equiv -c \frac{d\tau_o}{dt} \exp(-c\tau_o), \quad (\text{B.10})$$

gives the probability that a photon last scattered at time t (\bar{T}) when the temperature was \bar{T} , where

$$\tau_o(t) \equiv \int_{t(\bar{T})}^{t_0} \sigma_T \bar{n}_e dt \quad (\text{B.11})$$

is the *optical depth*, σ_T being the Thomson scattering cross-section, and $\bar{n}_e = \bar{n}_p$ the free electron density. The maximum of the visibility function then defines the photon last scattering surface at t_{dec} .

Acoustic fluctuations in baryons are frozen in slightly later at the baryon drag epoch [35] defined by the condition $c\tau_d \simeq 1$, where

$$\tau_d(t) \equiv \int_t^{t_0} \frac{\dot{\tau}_o dt}{\bar{a}R} = \int_t^{t_0} \frac{\sigma_T \bar{n}_e dt}{\bar{a}R} \quad (\text{B.12})$$

is the *drag depth* and $R \equiv 0.75\rho_B/\rho_\gamma = 0.75(\bar{\Omega}_{B0}\bar{a})/(\bar{\Omega}_{\gamma0}\bar{a}_0)$.

References

- [1] Hoyle F and Vogeley M S 2002 *Astrophys. J.* **566** 641
- [2] Hoyle F and Vogeley M S 2004 *Astrophys. J.* **607** 751
- [3] Pan D C, Vogeley M S, Hoyle F, Choi Y-Y and Park C 2012 *Mon. Not. R. Astr. Soc.* **421** 926
- [4] Ellis G F R 1984 *General Relativity and Gravitation*, eds. B Bertotti, F de Felice and A Pascolini, (Dordrecht: Reidel) pp 215-288
- [5] Ellis G F R and Stoeger W 1987 *Class. Quantum Grav.* **4** 1697
- [6] Wiltshire D L 2011 *Class. Quantum Grav.* **28** 164006
- [7] Buchert T 2011 *Class. Quantum Grav.* **28** 164007
- [8] Clarkson C, Ellis G F R, Larena J and Umeh O 2011 Rept. Prog. Phys. **74** 112901
- [9] van den Hoogen R J 2012 *Proceedings of the 12th Marcel Grossmann Meeting on General Relativity*, eds. T Damour, R T Jantzen and R Ruffini, (Singapore: World Scientific) pp 578-589
- [10] Buchert T and Räsänen S 2012 *Ann. Rev. Nucl. Part. Sci.* **62** 57
- [11] Wiltshire D L 2007 *New J. Phys.* **9** 377
- [12] Wiltshire D L 2007 *Phys. Rev. Lett.* **99** 251101
- [13] Wiltshire D L 2009 *Phys. Rev. D* **80** 123512
- [14] Leith B M, Ng S C C and Wiltshire D L 2008 *Astrophys. J.* **672** L91
- [15] Smale P R and Wiltshire D L 2011 *Mon. Not. R. Astr. Soc.* **413** 367.
- [16] Smale P R 2011 *Mon. Not. R. Astr. Soc.* **418** 2779
- [17] Buchert T 2000 *Gen. Relativ. Grav.* **32** 105

- [18] Buchert T 2001 *Gen. Relativ. Grav.* **33** 1381
- [19] Buchert T and Carfora M 2002 *Class. Quantum Grav.* **19** 6109
- [20] Buchert T and Carfora M 2003 *Phys. Rev. Lett.* **90** 031101
- [21] Wiltshire D L 2008 *Phys. Rev. D* **78** 084032
- [22] Viaggiu S 2012 *Class. Quantum Grav.* **29** 035016
- [23] Viaggiu S and Montuori M 2013 *Int. J. Mod. Phys. D* **22** 1350065
- [24] Cyburt R H, Fields B D and Olive K A 2008 *J. Cosmol. Astropart. Phys.* JCAP 11 (2008) 012
- [25] Tytler D D, O'Meara J M, Suzuki N and Lubin D 2000 *Phys. Scripta* **T 85**, 12
- [26] Steigman G 2006 *Int. J. Mod. Phys. E* **15**, 1
- [27] Ade P A R *et al* 2013 arXiv:1303.5076.
- [28] Kessler R *et al* 2009 *Astrophys. J. Suppl.* **185**, 32
- [29] Riess A G *et al* 2011 *Astrophys. J.* **730**, 119; (E) **732**, 129
- [30] Wiltshire D L, Smale P R, Mattsson T and Watkins R 2012 arXiv:1201.5371
- [31] Rubart M and Schwarz D J 2013 arXiv:1301.5559
- [32] Weinberg S 2008 *Cosmology*, (New York: Oxford University Press) pp 113-129
- [33] Peebles P J E 1968 *Astrophys. J.* **153** 1
- [34] Seager S, Sasselov D D and Scott D 1999 *Astrophys. J.* **523** L1
- [35] Hu W and Sugiyama N 1996 *Astrophys. J.* **471** 542